Evidence for a Square-Square Vortex Lattice Transition in a High-T_c Cuprate Superconductor

D. J. Campbell,[1] M. Frachet,[1] S. Benhabib,[1] I. Gilmutdinov,[1] C. Proust,[1] T. Kurosawa,[2] N. Momono,[3] M. Oda,[2] M. Horio,[4] K. Kramer,[4] J. Chang,[4] M. Ichioka,[5] and D. LeBoeuf[1,*]

[1]*LNCMI-EMFL, CNRS UPR3228, Université Grenoble Alpes, Université de Toulouse, Université de Toulouse 3, INSA-T, Grenoble and Toulouse, France*

[2]*Department of Physics, Hokkaido University, Sapporo 060-0810, Japan*

[3]*Muroran Institute of Technology, Muroran 050-8585, Japan*

[4]*Physik-Institut, Universität Zürich, Winterthurerstrasse 190, CH-8057 Zürich, Switzerland*

[5]*Research Institute for Interdisciplinary Science, Okayama University, Okayama 700-8530, Japan*

(Received 16 November 2021; revised 1 March 2022; accepted 27 June 2022; published 2 August 2022)

Using sound velocity and attenuation measurements in high magnetic fields, we identify a new transition in the vortex lattice state of $La_{2-x}Sr_xCuO_4$. The transition, observed in magnetic fields exceeding 35 T and temperatures far below zero field T_c, is detected in the compression modulus of the vortex lattice, at a doping level of $x = p = 0.17$. Our theoretical analysis based on Eilenberger's theory of the vortex lattice shows that the transition corresponds to the long-sought 45° rotation of the square vortex lattice, predicted to occur in d-wave superconductors near a van Hove singularity.

DOI: 10.1103/PhysRevLett.129.067001

The band structure of 2D metals hosts special points, known as van Hove singularities (vHS), where the density of states diverges. When the Fermi level is tuned toward a vHS, electronic correlations are amplified. This is exemplified in twisted bilayer graphene, where proximity to a vHS at certain "magic angles" [1] can stabilize unconventional superconductivity [2] and correlated insulating states [3]. In Sr_2RuO_4 a vHS can be tuned to the Fermi level with chemical substitution or strain, yielding a dramatic increase of superconducting T_c [4], and non-Fermi liquid behavior [5,6]. Finally, in high-T_c cuprate superconductors, the closing of the notorious pseudogap has been associated with doping through a vHS [7].

In 2D type-II superconductors with d-wave gap symmetry, the proximity to a vHS results in unique behavior of the vortex lattice (VL). Generally, at low enough fields, a triangular vortex lattice minimizes the dominant electromagnetic interactions [8]. With increasing field, the intervortex distance decreases and anisotropies in the electronic structure and/or superconducting gap become relevant. They produce anisotropic screening currents and field distributions around vortices that lead to solid-solid transitions where the symmetry and orientation of the VL with respect to the crystallographic axes are modified. Such solid-solid transitions are of central interest in a wide variety of fields beyond superconductivity, such as metallurgy and crystallography [9].

In $YBa_2Cu_3O_y$, the d-wave gap anisotropy is dominant. Consequently, a square VL with nearest neighbors along the nodal direction is expected [10], as observed with small angle neutron scattering (SANS) [11,12]. On the other hand, in $La_{2-x}Sr_xCuO_4$ (LSCO) close to optimal doping, proximity to a vHS induces a significant Fermi velocity (v_F) anisotropy that in turn stabilizes a square VL with nearest-neighbor direction oriented along the Cu—O bond at low field [13,14].

The presence of a d-wave gap and fourfold Fermi velocity anisotropy are the ingredients of a long-standing theoretical prediction. Using the Eilenberger theory of the VL [15], Nakai *et al.* predicted that in a sufficiently large magnetic field, the vortex lattice will rotate 45°, through a first order phase transition, changing the nearest-neighbor vortex alignment from along the minima in v_F to the minima in the superconducting gap Δ. It is thus predicted that eventually, as the upper critical field is approached, the superconducting gap anisotropy dictates the square lattice coordination [16].

The d-wave superconductor LSCO near its doping-induced Lifshifz transition is a promising candidate material to display such physics. However, the unconventional electronic properties that typify high-T_c cuprates call into question the applicability of conventional theories for vortex physics. The prediction of a field-induced square-square vortex lattice rotation thus stands as an important test of such theories. Experimentally, however, this is a challenging task. Scanning tunneling microscopy, traditionally used to image the VL [17], is not applicable to LSCO as high quality surfaces have not been established. The weak neutron-matter interaction requires SANS experiments to be carried out using dc magnets to obtain sufficient counting statistics. This fact has prevented SANS from accessing field strengths of interest. Ultrasound offers

a solution to all those challenges: it is sensitive to the elasticity of the VL and can be measured in pulsed magnetic fields, which cover a larger field range.

Here we present an ultrasound study of the VL of LSCO up to 65 T and down to 1.5 K. We find a new elastic anomaly, marked by a sudden jump in the sound velocity at low temperatures. Measuring doping levels from $p = 0.10$ to $p = 0.215$, we see it only at $p = 0.17$ ($T_c = 38$ K). Moreover, the transition is only observed in the in-plane compression mode, leaving other modes unaffected. Given the absence of any sharp electronic phase transition in this temperature-field range, and the fact that the transition is only seen within the VL state, we conclude that the feature can only come from a change in the VL structure. Using Eilenberger equations along with a realistic tight-binding model of the electronic structure of LSCO $p = 0.17$, we show that a square-square first order transition is expected in the field and temperature range where the ultrasound anomalies are observed. We hence conclude that the transition detected in ultrasound in LSCO $p = 0.17$ is the long-sought square-square VL transformation.

The elastic tensor of a triangular VL is made up of three independent elastic moduli (assuming a field along the c axis): a compression modulus $c_L^v = c_{11}^v - c_{66}^v$, a tilt modulus c_{44}^v, and a shear modulus c_{66}^v (Voigt notation used; see Refs. [18,19] for reviews). In the field range considered here, and for extreme type-II superconductors such as LSCO ($\kappa \approx 100$), we have $c_{66}^v \ll c_{11}^v = c_{44}^v \approx B^2/4\pi$ [18]. In the following we discuss the VL properties of LSCO $p = 0.17$ which has square coordination for $B > 0.4$ T [13,14]. In contrast to the triangular VL, the square VL has four independent moduli, and the compression modulus is $c_L^v = (c_{11}^v + c_{12}^v)/2$.

Pinning of the flux lines is responsible for the coupling between the crystal lattice and the VL. When the VL is pinned, the sound velocity v_s has an additional contribution Δc_{ij}^v from the VL: $\rho v_s^2 = c_{ij}^c + \Delta c_{ij}^v$, with ρ the mass density and c_{ij}^c the crystal lattice elastic modulus. In the early 90s, Pankert *et al.* developed a phenomenological model based on thermally assisted flux flow (TAFF) to describe the influence of the VL on the ultrasound properties in cuprate superconductors [20]. The model has been successfully applied to several cuprates, including LSCO [21–23]. Within this model, Δc_{ij}^v is given by the VL elastic moduli c_{ij}^v, renormalized by the VL dynamics associated with the TAFF model.

Data in the c_{11} mode of LSCO $p = 0.17$ at 2.2 K (Fig. 1) illustrate the expected behavior as a function of the magnetic field (see the Supplemental Material [24] for measurement setup and sample characterization). With the field along the c axis, this mode probes the compression modulus of the VL (Table SII in the Supplemental Material [24]). At low fields, the VL is pinned, and the sound velocity follows the B^2 increase of the VL compression

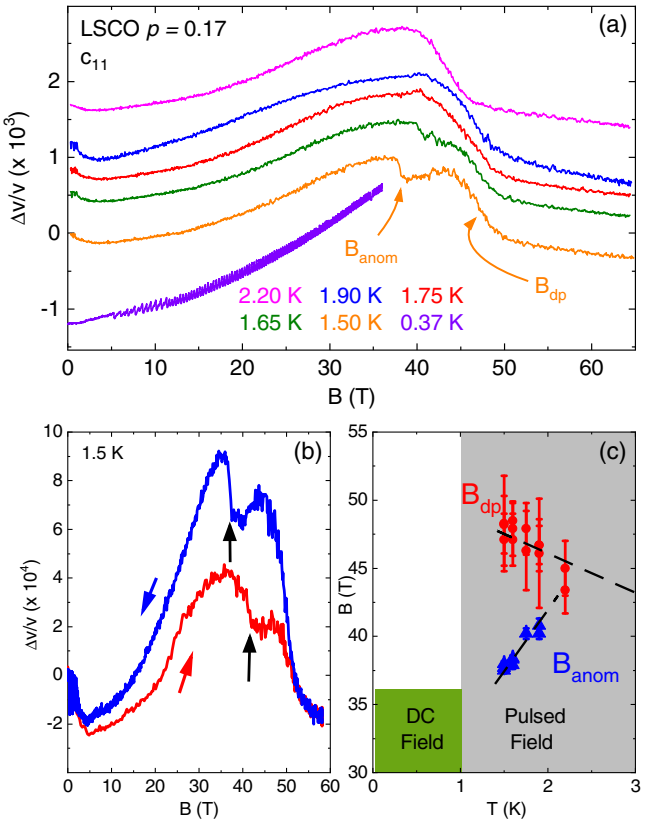

FIG. 1. (a) The change in sound velocity of the in-plane longitudinal mode (called c_{11}) of a LSCO $p = 0.17$ crystal at different temperatures, as a function of field applied along the c axis. All data are from pulsed field downsweeps, except the lowest temperature curve which is an upsweep in a DC field magnet. This curve shows a series of spikes above 5 T or so, associated with flux jumps. Curves have been offset vertically (though not by a constant amount). The arrows mark the field of the anomaly, B_{anom}, which is visible but more subtle up to 1.90 K in the sound velocity, and the depinning field B_{dp}. Measurements were taken at frequencies of 155 MHz in pulsed field and 127 MHz in DC field. (b) Sound velocity of the c_{11} mode at 1.5 K. The upsweep (downsweep) is shown in red (blue). For increasing fields, the VL transition is found at 41 T while it appears at 37 T or so for decreasing fields, as indicated by the black arrows. The fact that above the irreversibility field the two curves overlap and that the depinning field is identical for both upsweeps and downsweeps shows isothermal conditions during the magnetic field pulse. (c) Temperature-magnetic field phase diagram, showing the area covered by ultrasound measurements in different magnet systems and the location of the anomaly during downsweeps (blue) and vortex melting (red). Dashed lines are guides to the eye.

modulus. At 40 T or so, a steplike decrease is observed in the sound velocity. It corresponds to the depinning of the VL which results in the loss of the VL contribution to the sound velocity. The ultrasound attenuation $\Delta\alpha(B)$ [Fig. S1(a) in the Supplemental Material [24]] shows a broad peak at this depinning field, as also expected within the TAFF model.

Below 2 K we see another elastic anomaly emerge, in the form of a smaller but more sudden dip at 1.5 K just below 40 T, and a more subtle change in the signal through 1.9 K [see derivative of $\Delta v/v$ with respect to B in Fig. S1(b) of the Supplemental Material [24] where the anomaly is more visible throughout the temperature range]. The field at which this feature appears also slightly increases, up to about 43 T. There is a small uptick in the attenuation at the same field [24]. The new elastic anomaly shows hysteretic behavior between the upsweep and downsweep of the field pulse [Fig. 1(b)]. The phase diagram in Fig. 1(c) shows the field of this feature [B_{anom}, defined as the dip in the derivative shown in Fig. S1(b) in the Supplemental Material [24]], as well as the vortex depinning line [B_{dp}, defined as the peak in $\Delta\alpha(B)$ Fig. S1(a) in the Supplemental Material [24]]. Though the trend line would make it seem as if the anomaly should be observed at a lower field and lower temperature, no similar behavior was seen down to 0.37 K in DC field measurements up to 36 T on the same sample. This surprising observation has a natural explanation that will be given later.

Although we investigated other elastic modes for a similar anomaly, it is only present in c_{11}. Figure 2(a) shows a comparison of c_{11} to two other configurations at 1.5 K, neither of which shows an anomaly. We have also measured the c_{11} mode of other dopings of LSCO (Fig. S4 in the Supplemental Material [24]). All are qualitatively similar, with an increase in the mixed state and dropoff at their corresponding B_{dp}. However, the only one with an anomaly before the depinning field is $p = 0.17$, establishing the uniqueness of this doping.

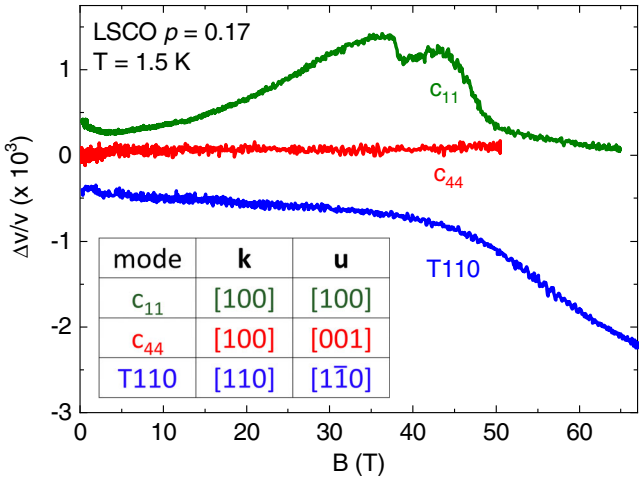

FIG. 2. A comparison of the field dependence of three different ultrasound modes in LSCO $p = 0.17$, taken at 1.5 K, from downsweeps in pulsed field measurements. The table shows the propagation **k** and polarization **u** directions for different modes. The different elastic constants of the square and hexagonal VL probed for different propagation and polarization directions used here are listed in Table SII in the Supplemental Material [24]. We have also probed the $L110$ mode of LSCO $p = 0.17$, but the signal in this configuration is strongly attenuated below the high temperature tetragonal-low temperature orthorhombic (HTT-LTO) structural transition, resulting in a poor signal-to-noise ratio and preventing us from detecting an anomaly (Fig. S2 in the Supplemental Material [24]).

In LSCO $p = 0.17$, a spin glass is present in high magnetic fields; it is characterized by a gradual slowing down of spin fluctuations that produces the smooth softening of the $T110$ mode (Fig. 2) [31,32]. The new sharp feature observed in the c_{11} mode is consequently unlikely to be related to this gradual magnetic freezing. Moreover, the transition is only observed in the in plane compression mode c_{11}, suggesting it is not a structural transition of the crystal lattice. Instead, it is what we expect for a transition in the vortex lattice, as c_{11} is the most sensitive mode to the VL elasticity. It measures the compression modulus of the VL, whereas the c_{44} mode does not couple to the VL, and $T110$ probes the VL shear modulus c_{66}^{v} (see Table SII in the Supplemental Material [24]), the value of which is well below our resolution. All these observations, along with the fact that the new feature only exists within the pinned vortex solid phase bounded by the red points in Fig. 1(b), suggest that the new anomaly has its origin in VL physics.

Since the vortex depinning field is unchanged with the appearance of the feature, an ordered and pinned VL is presumably still present above B_{anom}, with only its elasticity or coupling to the crystal lattice being modified. The transition is remarkably sharp, with indication of hysteresis as shown in Fig. 1(b), pointing to a first order phase transition. The most likely explanation is a structural transformation of the VL. Ultrasound should be sensitive to such transitions, which are expected to involve either a change in elasticity or pinning strength. Indeed, ultrasound has been used to observe such VL transitions in YNi_2B_2C [33]. As discussed above, the interplay between a superconducting gap and v_F taking place in LSCO results in a square VL configuration with nearest-neighbor direction aligned along the Cu—O directions at low fields [13,14,34]. Earlier calculations based on Eilenberger's theory predicted that, at higher fields, this interplay leads to further transformation: the $\square_v$ can either transition to a hexagonal lattice, or to a gap-centered square lattice $\square_g$—the latter being, in essence, a 45° rotation [16].

To identify the nature of the VL transition and since the work of Ref. [16] was based on parameters found in borocarbides, we have performed our own calculation using 2D tight-binding model parameters specific to LSCO $p = 0.17$ obtained via angle-resolved photoemission spectroscopy [24,35]. We evaluate the free energy for a given VL shape, after calculating the vortex state with Eilenberger's theory [24]. From the condition that the free energy increases with a small deformation of the square VL, we can determine the regions [denoted A–D in Fig. 3(b)] where the $\square_v$ and $\square_g$ VL are stable. At low temperature and field (regions C and D) the $\square_v$ VL is favored, as observed in prior experiment [13]. At higher

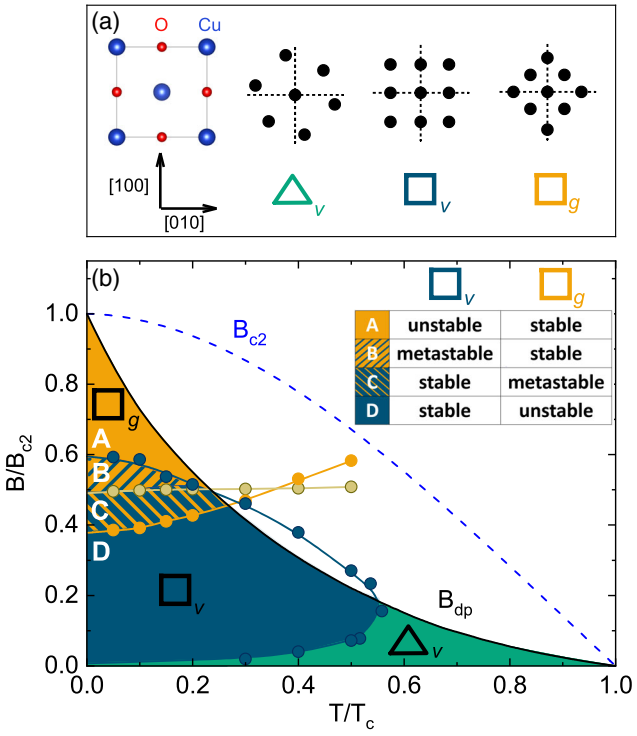

FIG. 3. (a) Left: the Cu—O plane [37] of LSCO, with the c axis out of the page. Right: illustrations of the hexagonal, v_F-centered square and superconducting gap-centered square vortex lattices, respectively, relative to the crystal lattice, with vortices portrayed as black circles. Dashed lines mark the Cu—O—Cu bond directions, also the [100] axes of the high temperature tetragonal phase. (b) A phase diagram for $p = 0.17$ showing the calculated VL configurations as a function of T and B. The hexagonal phase is stable in the green-colored region at high T, low B. In regions A and D (orange and blue), one of the two square lattices is stable. The brown line (B-C boundary) marks the transition between the two square VL arrangements in slowly varying magnetic field. Metastable regions B and C emerging in pulsed fields are shown with slashed lines. The vortex solid is unobservable with ultrasound for $B > B_{dp}$. Solid circles are results of the calculation, and lines connecting them are guides to the eye. The depinning transition was not taken into account for the calculations.

fields (regions A and B), the contribution of the Fermi surface anisotropy becomes weaker, and the influence of the gap structure favors a $\square_g$ VL orientation [16]. Because the reorientation is a first order transition, VL configurations can have a wide range of metastability within which they can resist temperature or field fluctuations before transitioning to the more energetically favorable configuration [36]. Consequently, in regions B (C) the unfavored $\square_v$ ($\square_g$) VL can exist in a metastable state. This means that for downsweeps of pulsed field measurements such as shown in Fig. 1, the $\square_g$ VL configuration survives in region C until it undergoes a first order transition to the $\square_v$ VL at the C-D boundary (orange circles in Fig. 3). In contrast, in static field measurements, where magnetic field is swept more slowly, the transition is expected at a higher field, at the B-C boundary (brown circles).

The theory qualitatively explains the absence of any transition in the dc field measurements. It should only be found at fields above $B_{\rm anom}$ obtained from pulsed field downsweeps. In contrast with Ref. [16] which found a reentrant hexagonal phase at low T between the two square VL configurations, our calculation yields a single, first order transition in LSCO $p = 0.17$ at low T, as observed experimentally. As noted, a comparison of the upsweeps and downsweeps of the field pulse shows evidence for hysteresis [Fig. 1(b)], indicating the first order character of the transition. The C-D boundary increases in field with T, as does $B_{\rm anom}$. The overall qualitative agreement between theory and experiment is remarkable, and we hence conclude that the ultrasound anomaly at $B_{\rm anom}$ in LSCO $p = 0.17$ corresponds to a square-square VL transition. There is, however, some discrepancy between the transition field predicted by theory (C-D boundary at $B/B_{c2} \approx 0.4$ at low T) and the measured $B_{\rm anom}/B_{c2} \approx 0.7$ at 1.5 K, with $B_{c2} = 55$ T [31]. This difference can be explained by at least two factors. First, the theoretical curve of B_{c2} may be suppressed at low temperatures if paramagnetic pair breaking and competing electronic orders are considered. Second, including the c-axis dispersion in the tight-binding model for LSCO may quantitatively shift the C-D boundary [38]. Further theoretical work could resolve this discrepancy, and novel theoretical methods such as molecular dynamics models could provide new insights into this square-square transition [39,40].

Our data show that the sound velocity in the $\square_g$ VL is smaller than in the $\square_v$ VL. This difference can either be due to a smaller rigidity of the $\square_g$ VL or enhanced pinning of the $\square_v$ VL. Note that we do not observe the hexagonal-to-$\square_v$ transition previously reported for $p > 0.145$ using SANS. For $p = 0.17$ this transition occurs at $B \approx 0.4$ T [14], where the vortex contribution to sound velocity change is small and any anomaly associated with a transition is thus below the measurement resolution $\Delta v/v \sim 10^{-6}$. Our extensive doping dependence (Fig. S4 in the Supplemental Material [24]) shows that the $\square_v$-$\square_g$ transition only exists within a limited doping range around $p = 0.17$. One of the prerequisites for the VL transition to occur is the existence of a sufficiently ordered VL in high fields. It is plausible that this condition is only found around $p = 0.17$. A disordered VL has been found for doping levels $p \leq 0.145$ where the spin glass phase stabilized at low fields acts as a source of disorder for the VL [14]. Furthermore, in LSCO $p = 0.215$, our ultrasound data show signatures of a fishtail effect, suggesting the presence of a disordered VL at this doping level. As discussed in more detail in the Supplemental Material [24], the field dependence of the sound velocity at $p = 0.215$ in a dc magnetic field shows a broad maximum for $B < B_{\rm dp}$, which is reminiscent of the second magnetization peak

[41]. We note that this feature is absent in LSCO $p = 0.17$ as can be seen in Fig. 1(a), showing that (i) our LSCO $p = 0.17$ sample does not harbor the order-disorder transition presumably underpinning the fishtail effect and (ii) an ordered VL exists up to B_{dp} in our LSCO $p = 0.17$ sample.

In summary, we have conducted an ultrasound study of LSCO at several hole concentrations, measuring different elastic modes at low temperature in both pulsed and dc magnetic fields. For $p = 0.17$, we observe a novel feature in the c_{11} mode deep within the mixed phase. Motivated by theoretical calculations based on Eilenberger equations, we interpret this ultrasound elastic anomaly in terms of a 45° square VL rotation. Requiring a unique combination of d-wave superconductivity and proximity to a van Hove singularity, this square-square transition is not as widespread as the lower field rhombic-square transition [11–14,17,33]. Even in LSCO, a material that meets both these requirements, the VL transition only exists in a restricted range of doping. That being said, our results provide experimental evidence of the long-standing Eilenberger theory prediction of a magnetic-field-induced square-square VL transition.

We thank E. M. Forgan, K. Machida, and M.-H. Julien for valuable discussions. Part of this work was performed at the LNCMI-CNRS, a member of the European Magnetic Field Laboratory (EMFL). Work at LNCMI. was supported by the Laboratoire d'Excellence LANEF (ANR-10-LABX-51-01), French Agence Nationale de la Recherche (ANR) Grant No. ANR-19-CE30-0019-01 (Neptun) and EUR Grant No. NanoX nANR-17-EURE-0009. M. H., K. K., and J. C. acknowledge support by the Swiss National Science Foundation.

*david.leboeuf@lncmi.cnrs.fr

[1] N. Yuan, H. Isobe, and L. Fu, Magic of high-order van Hove singularity, Nat. Commun. **10**, 5769 (2019).

[2] Y. Cao, V. Fatemi, S. Fang, K. Watanabe, T. Taniguchi, E. Kaxiras, and P. Jarillo-Herrero, Unconventional superconductivity in magic-angle graphene superlattices, Nature (London) **556**, 43 (2018).

[3] Y. Cao, V. Fatemi, A. Demir, S. Fang, S. L. Tomarken, J. Y. Luo, J. D. Sanchez-Yamagishi, K. Watanabe, T. Taniguchi, E. Kaxiras *et al.*, Correlated insulator behaviour at half-filling in magic-angle graphene superlattices, Nature (London) **556**, 80 (2018).

[4] C. W. Hicks, D. O. Brodsky, E. A. Yelland, A. S. Gibbs, J. A. Bruin, M. E. Barber, S. D. Edkins, K. Nishimura, S. Yonezawa, Y. Maeno, and A. P. Mackenzie, Strong increase of T_c of Sr_2RuO_4 under both tensile and compressive strain, Science **344**, 283 (2014).

[5] B. Burganov, C. Adamo, A. Mulder, M. Uchida, P. D. C. King, J. W. Harter, D. E. Shai, A. S. Gibbs, A. P. Mackenzie, R. Uecker, M. Bruetzam, M. R. Beasley, C. J. Fennie, D. G. Schlom, and K. M. Shen, Strain Control of Fermiology and Many-Body Interactions in Two-Dimensional Ruthenates, Phys. Rev. Lett. **116**, 197003 (2016).

[6] M. E. Barber, A. S. Gibbs, Y. Maeno, A. P. Mackenzie, and C. W. Hicks, Resistivity in the Vicinity of a van Hove Singularity: Sr_2RuO_4 under Uniaxial Pressure, Phys. Rev. Lett. **120**, 076602 (2018).

[7] S. Benhabib, A. Sacuto, M. Civelli, I. Paul, M. Cazayous, Y. Gallais, M.-A. Méasson, R. D. Zhong, J. Schneeloch, G. D. Gu, D. Colson, and A. Forget, Collapse of the Normal-State Pseudogap at a Lifshitz Transition in the $Bi_2Sr_2CaCu_2O_{8+\delta}$ Cuprate Superconductor, Phys. Rev. Lett. **114**, 147001 (2015).

[8] W. H. Kleiner, L. M. Roth, and S. H. Autler, Bulk solution of Ginzburg-Landau equations for type II superconductors: Upper critical field region, Phys. Rev. **133**, A1226 (1964).

[9] Y. Peng, W. Li, F. Wang, T. Still, A. Yodh, and Y. Han, Diffusive and martensitic nucleation kinetics in solid-solid transitions of colloidal crystals, Nat. Commun. **8**, 14918 (2017).

[10] M. Ichioka, A. Hasegawa, and K. Machida, Field dependence of the vortex structure in d-wave and s-wave superconductors, Phys. Rev. B **59**, 8902 (1999).

[11] B. Keimer, W. Y. Shih, R. W. Erwin, J. W. Lynn, F. Dogan, and I. A. Aksay, Vortex Lattice Symmetry and Electronic Structure in $YBa_2Cu_3O_7$, Phys. Rev. Lett. **73**, 3459 (1994).

[12] S. P. Brown, D. Charalambous, E. C. Jones, E. M. Forgan, P. G. Kealey, A. Erb, and J. Kohlbrecher, Triangular to Square Flux Lattice Phase Transition in $YBa_2Cu_3O_7$, Phys. Rev. Lett. **92**, 067004 (2004).

[13] R. Gilardi, J. Mesot, A. Drew, U. Divakar, S. L. Lee, E. M. Forgan, O. Zaharko, K. Conder, V. K. Aswal, C. D. Dewhurst *et al.*, Direct Evidence for an Intrinsic Square Vortex Lattice in the Overdoped High- T_c Superconductor $La_{1.83}Sr_{0.17}CuO_{4+\delta}$, Phys. Rev. Lett. **88**, 217003 (2002).

[14] J. Chang, J. S. White, M. Laver, C. J. Bowell, S. P. Brown, A. T. Holmes, L. Maechler, S. Strässle, R. Gilardi, S. Gerber *et al.*, Spin density wave induced disordering of the vortex lattice in superconducting $La_{2-x}Sr_xCuO_4$, Phys. Rev. B **85**, 134520 (2012).

[15] G. Eilenberger, Transformation of Gorkov's equation for type II superconductors into transport-like equations, Z. Phys. A **214**, 195 (1968).

[16] N. Nakai, P. Miranović, M. Ichioka, and K. Machida, Reentrant Vortex Lattice Transformation in Fourfold Symmetric Superconductors, Phys. Rev. Lett. **89**, 237004 (2002).

[17] B. B. Zhou, S. Misra, E. H. da Silva Neto, P. Aynajian, R. E. Baumbach, J. Thompson, E. D. Bauer, and A. Yazdani, Visualizing nodal heavy fermion superconductivity in $CeCoIn_5$, Nat. Phys. **9**, 474 (2013).

[18] A. Campbell and J. Evetts, Flux vortices and transport currents in type II superconductors, Adv. Phys. **21**, 199 (1972).

[19] E. H. Brandt, The flux-line lattice in superconductors, Rep. Prog. Phys. **58**, 1465 (1995).

[20] J. Pankert, Ultrasonic attenuation in the mixed state of high-tc superconductors, Physica (Amsterdam) **168C**, 335 (1990).

[21] J. Pankert, G. Marbach, A. Comberg, P. Lemmens, P. Fröning, and S. Ewert, Ultrasonic Attenuation by the Vortex

Lattice of High-T_c Superconductors, Phys. Rev. Lett. **65**, 3052 (1990).

[22] P. Lemmens, P. Frning, S. Ewert, J. Pankert, G. Marbach, and A. Comberg, Ultrasonic attenuation by the vortex lattice of $Bi_{1.6}Pb_{0.4}Sr_2Ca_2Cu_3O_y$, Physica (Amsterdam) **174C**, 289 (1991).

[23] T. Hanaguri, T. Fukase, I. Tanaka, and H. Kojima, Elastic properties and anisotropic pinning of the flux-line lattice in single-crystalline $La_{1.85}Sr_{0.15}CuO_4$, Phys. Rev. B **48**, 9772 (1993).

[24] See Supplemental Material at http://link.aps.org/supplemental/10.1103/PhysRevLett.129.067001 for additional data and experimental and theoretical details, which includes Refs. [25–30].

[25] J. Chang, C. Niedermayer, R. Gilardi, N. B. Christensen, H. M. Rønnow, D. F. McMorrow, M. Ay, J. Stahn, O. Sobolev, A. Hiess, S. Pailhes, C. Baines, N. Momono, M. Oda, M. Ido, and J. Mesot, Tuning competing orders in $La_{2-x}Sr_xCuO_4$ cuprate superconductors by the application of an external magnetic field, Phys. Rev. B **78**, 104525 (2008).

[26] M. Nohara, T. Suzuki, Y. Maeno, T. Fujita, I. Tanaka, and H. Kojima, Unconventional lattice stiffening in superconducting $La_{2-x}Sr_xCuO_4$ single crystals, Phys. Rev. B **52**, 570 (1995).

[27] K. M. Suzuki, K. Inoue, P. Miranovi, M. Ichioka, and K. Machida, Generic first-order orientation transition of vortex lattices in type II superconductors, J. Phys. Soc. Jpn. **79**, 013702 (2010).

[28] Y. Sera, T. Ueda, H. Adachi, and M. Ichioka, Relation of superconducting pairing symmetry and non-magnetic impurity effects in vortex states, Symmetry **12**, 175 (2020).

[29] C. Cura, J. Pal, R. Schubert, S. Ewert, G. Fuchs, and G. Krabbes, Magnetostriction and magnetoacoustic measurements on pure and Zn-doped YBCO crystals, Physica (Amsterdam) **388-389C**, 261 (2003), proceedings of the 23rd International Conference on Low Temperature Physics (LT23).

[30] D. Miu, T. Noji, T. Adachi, Y. Koike, and L. Mi u, On the nature of the second magnetization peak in $FeSe_{1-x}Te_x$ single crystals, Supercond. Sci. Technol. **25**, 115009 (2012).

[31] M. Frachet *et al.*, Hidden magnetism at the pseudogap critical point of a cuprate superconductor, Nat. Phys. **16**, 1064 (2020).

[32] M. Frachet, S. Benhabib, I. Vinograd, S.-F. Wu, B. Vignolle, H. Mayaffre, S. Krämer, T. Kurosawa, N. Momono, M. Oda, J. Chang, C. Proust, M.-H. Julien, and D. LeBoeuf, High magnetic field ultrasound study of spin freezing in $La_{1.88}Sr_{0.12}CuO_4$, Phys. Rev. B **103**, 115133 (2021).

[33] S. Ishikawa and T. Watanabe, Ultrasound velocity measurements in the vortex-state of YNi_2B_2C, J. Phys. Conf. Ser. **391**, 012023 (2012).

[34] A. Drew, D. Heron, U. Divakar, S. Lee, R. Gilardi, J. Mesot, F. Ogrin, D. Charalambous, N. Momono, M. Oda *et al.*, μSR measurements on the vortex lattice of $La_{1.83}Sr_{0.17}CuO_4$, Physica (Amsterdam) **374-375B**, 203 (2006).

[35] J. Chang, M. Shi, S. Pailhés, M. Månsson, T. Claesson, O. Tjernberg, A. Bendounan, Y. Sassa, L. Patthey, N. Momono, M. Oda, M. Ido, S. Guerrero, C. Mudry, and J. Mesot, Anisotropic quasiparticle scattering rates in slightly underdoped to optimally doped high-temperature $La_{2-x}Sr_xCuO_4$ superconductors, Phys. Rev. B **78**, 205103 (2008).

[36] E. R. Louden, C. Rastovski, L. DeBeer-Schmitt, C. D. Dewhurst, N. D. Zhigadlo, and M. R. Eskildsen, Nonequilibrium structural phase transitions of the vortex lattice in MgB_2, Phys. Rev. B **99**, 144515 (2019).

[37] K. Momma and F. Izumi, *VESTA3* for three-dimensional visualization of crystal, volumetric and morphology data, J. Appl. Crystallogr. **44**, 1272 (2011).

[38] M. Horio, K. Hauser, Y. Sassa, Z. Mingazheva, D. Sutter, K. Kramer, A. Cook, E. Nocerino, O. K. Forslund, O. Tjernberg *et al.*, Three-Dimensional Fermi Surface of Overdoped La-Based Cuprates, Phys. Rev. Lett. **121**, 077004 (2018).

[39] M. W. Olszewski, M. R. Eskildsen, C. Reichhardt, and C. J. O. Reichhardt, Structural transitions in vortex systems with anisotropic interactions, New J. Phys. **20**, 023005 (2018).

[40] M. W. Olszewski, M. R. Eskildsen, C. Reichhardt, and C. J. O. Reichhardt, Rotational transition, domain formation, dislocations, and defects in vortex systems with combined sixfold and twelvefold anisotropic interactions, Phys. Rev. B **101**, 224504 (2020).

[41] Y. Tanabe, T. Adachi, K. Omori, H. Sato, T. Noji, and Y. Koike, Magnetic-field-induced enhancement of the vortex pinning in the overdoped regime of $La_{2-x}Sr_xCuO_4$: Relation to the microscopic phase separation, J. Phys. Soc. Jpn. **76**, 113706 (2007).